Received 9 May 2023, accepted 20 May 2023, date of publication 30 May 2023, date of current version 13 June 2023.
Digital Object Identifier 10.1109/ACCESS.2023.3281370

RESEARCH ARTICLE

Orbital Angular Momentum Mode Propagation and Supercontinuum Generation in a Soft Glass Bragg Fiber

AMOGH A. DYAVANGOUDAR[1], MAYUR KUMAR CHHIPA[2], ANKUR SAHARIA[1], (Member, IEEE), YASEERA ISMAIL[3], FRANCESCO PETRUCCIONE[4,5], ANTON V. BOURDINE[6,7,8], OLEG G. MOROZOV[9], (Senior Member, IEEE), VLADIMIR V. DEMIDOV[7], JUAN YIN[10], GHANSHYAM SINGH[11], (Senior Member, IEEE), AND MANISH TIWARI[1]

[1]Optoelectronics and Photonics Research Laboratory, Department of Electronics and Communication Engineering, Manipal University Jaipur, Jaipur 303007, India
[2]Department of Electronics and Communication Engineering, FICT, ISBAT University, Kampala, Uganda
[3]Quantum Research Group, School of Chemistry and Physics, University of KwaZulu-Natal, Durban 4001, South Africa
[4]School of Data Science and Computational Thinking, Stellenbosch University, Stellenbosch 7602, South Africa
[5]National Institute for Theoretical and Computational Sciences (NITheCS), Stellenbosch 7600, South Africa
[6]Department of Communication Lines, Povolzhskiy State University of Telecommunications and Informatics, 443010 Samara, Russia
[7]JSC "Scientific Production Association State Optical Institute named after Vavilov S. I.," 192171 Saint Petersburg, Russia
[8]Department of Photonics and Communication Links, Saint Petersburg State University of Telecommunications named after M. A. Bonch-Bruevich, 193232 Saint Petersburg, Russia
[9]Department of Radiophotonics and Microwave Technologies, Kazan National Research State University named after A. N. Tupolev-KAI, 420111 Kazan, Russia
[10]Division of Quantum Physics and Quantum Information, University of Science and Technology of China, Shanghai, Hefei 200093, China
[11]Department of ECE, Malaviya National Institute of Technology Jaipur, Jaipur 302017, India

Corresponding author: Mayur Kumar Chhipa (mayur.fict@isbatuniversity.com)

The work of Yaseera Ismail, Francesco Petruccione, Anton V. Bourdine, Juan Yin, Ghanshyam Singh, and Manish Tiwari was supported in part by the Russian Foundation for Basic Research (RFBR), Department of Science and Technology (DST), NSFC, and NRF under Project 19-57-80016 BRICSt; and in part by DST/ICD/BRICS/Call-3/Manish Tiwari-QuSaF/2019.

ABSTRACT This manuscript presents a ring-core Bragg Fiber (RC-BF) for orbital angular momentum (OAM) modes propagation and supercontinuum generation. The proposed RC-BF is composed of alternating layers of soft glasses SF57 and LLF1 to render high nonlinearity to the fiber. Mode analysis using full-vectorial finite element method resulted in obtaining HE/EH modes to support vector modes as well as orbital angular momentum modes. The optimized fiber supports 22 OAM modes and exhibits a zero-dispersion wavelength (ZDW). The small effective area of Fiber 3 aided in achieving the highest nonlinearity, $\gamma = 91.51\ \mathrm{W^{-1}km^{-1}}$. A near-infrared supercontinuum is generated with a 35 dB flatness over a bandwidth of ~1087 - 2024 nm in a 20 cm long RC-BF using a chirp-free hyperbolic secant pulse of width 200 fs and peak power of 5 kW.

INDEX TERMS Bragg fiber, finite element method, OAM modes, zero-dispersion wavelength, supercontinuum generation.

I. INTRODUCTION

Communication infrastructure connects servers, data centres and people around the world, and in the recent past, it has been accomplished largely due to optical networks. To overcome capacity issues that the current optical communication systems are facing, Space Division Multiplexing (SDM) is frequently utilized [1]. The research nowadays has piqued towards making sure that a huge number of modes are transmitted [2]. By multiplexing several orthogonal OAM modes, SDM employing orbital angular momentum (OAM) also holds the key for improving transmission capacity as well as spectrum efficiency [3], [4]. OAM beams possess a unique doughnut-shaped profile with a phase front of helical

The associate editor coordinating the review of this manuscript and approving it for publication was Muguang Wang.

nature given by exp($il\phi$), with the angle being represented by the azimuthal ϕ and the topological charge l. Stimulated Emission Depletion (STED) microscopy is an application of OAM which enables applications like super-resolution imaging where Gaussian and doughnut-shaped depletion beams are aligned [5]. The applications of OAM extend further in quantum communication [6], [7], optical trapping [8], [9] and sensing [10] etc.

When a laser beam propagates through a nonlinear medium, it undergoes spectral broadening. This process is called as supercontinuum generation [11]. It is clear from the GNLSE equation that it depends on the peak power as well as the nonlinear coefficient, fiber loss (which is necessary for dispersion), distance (fiber length) and time (pulse duration) [12]. Supercontinuum generation has found its applications in numerous broadband communication applications based on OCDMA [13], imaging through optical coherence tomography [14], [15], white light generation [16], chemical sensing and microscopy [17] etc.

Self Phase Modulation (SPM) generates an input pulse-centric, bell-shaped spectrum in conventional fibers. On the contrary, diverse effects such as SRS (stimulated Raman scattering), XPM (cross-phase modulation), GVD (group velocity dispersion), higher-order soliton generation, third-order dispersion, self-steeping and birefringence play significant role in the phenomenon of supercontinuum generation in photonic cystal fibers. [18]. Unlike conventional fibers, photonic crystal fibers acquire their characteristics from the air hole capillaries that are placed tightly throughout the fiber's length [19]. PCFs are preferred as they provide flexibility in designing of desired properties such as high nonlinearity and flat chromatic dispersion and their suitability for OAM mode transmission. Plethora of structures have been considered for OAM mode propagation such as hexagonal lattice PCF [20], circular PCF [21] and spiral shaped PCF [22]. Highly nonlinear PCFs are being designed either by modelling them with a very small effective area to have a tight mode confinement [23] or using materials that have very high intrinsic nonlinearity coefficients such as tellurites [24], [25], chalcogenides [26], [27] and lead silicate glasses [28], [29]. When a mode is tightly confined using these highly nonlinear materials, high values of γ are achieved. Supercontinuum generation has been previously demonstrated in speciality optical fibers such as in hollow core fibers filled with gases [30] and in all - normal dispersion fibers [31]. Further, Leong et al. [32], at 1.55 μm, have designed and fabricated a speciality optical fiber (PCF) for supercontinuum generation using soft glass lead silicate SF57 and have reported a very high nonlinearity, $\gamma = 1860$ W^{-1}km^{-1}. Agarwal et al. [33] have designed an ES-PCF using SF57 and have reported a nonlinearity of 2150 W^{-1}km^{-1} at 1.55 μm.

This work intended to present a ring-core Bragg Fiber designed using a combination of soft glasses available commercially by Schott, SF57 and LLF1. Bragg fibers are simpler to fabricate through the insertion of concentric arrangement of high-low index capillaries which forms the preform that can be drawn into fibers through fiber drawing process [34]. Nandam et al. [35] worked on a spiral shaped PCF with 12 arms and reported that the PCF sustained 14 OAM modes. However, due to the complexity of the structure, the fabrication of the structure becomes complex. Moreover, supercontinuum generation is not discussed for the structure. Wang et al. [36] propose a PCF with As_2S_3 and SiO_2 and report a wavelength of zero dispersion (ZDW) at 5300 nm. In this work, the proposed RC-BF comprises of two compatible nonlinear glasses with simpler structure in comparison to PCF and exhibit a ZDW near the telecommunication operating window of 1.55 μm and is optimized for OAM mode propagation and supercontinuum generation at 1.55 μm which serves as the pump wavelength. In the previous works, the focus has been on using the Bragg fiber either for OAM mode propagation [37] or supercontinuum generation [38]. In this work, both the OAM modes and the generation of supercontinuum spectrum have been demonstrated in the same Bragg fiber.

II. RING CORE- BRAGG FIBER DESIGN

A Full-vectorial Finite Element Method (FEM) is used for mode analysis and for the investigation of OAM modes in all three fibers using COMSOL Multiphysics. The schematic design of the proposed RC-BF is shown in Fig. 1. The fiber is designed in such a way that a ring core is encompassed by concentric arrangement of circles with alternating refractive indices. The concentric circles in the cladding region are arranged with an alternating high-low distribution of the refractive index. The central air hole radius is R = 2 μm. The exterior geometry is spread over a region of 6 circles with radii of R1 = 4.1 μm, R2 = 4.2 μm, R3 = 4.3 μm, R4 = 4.4 μm, R5 = 4.5 μm, R6 = 5 μm. The layers between R-R1 (core), R2-R3 and R4-R5 have a high linear refractive index material i.e. dense flint SF57 (n = 1.8015) while the material in the layers between R1-R2, R3-R4 and R5-R6 is low index very light flint LLF1 (n = 1.5286) at 1.55 μm. Both materials used in the design have a higher nonlinear refractive index in comparison to silica and low loss and are easier to fabricate in comparison to chalcogenides, tellurites, and other infrared glasses due to their high T_g (glass transition temperature) and low thermal expansion coefficient [39]. They are also thermally compatible, and their temperature characteristics are further shown in Table 1 [40].

TABLE 1. Temperature characteristics of Schott SF57 and Schott LLF1.

Glass	T_g (° C)	$T_{10}{}^{7.6}$ (° C)
Schott SF57	414	507
Schott LLF1	431	628

where, $T_{10}^{7.6}$ is the softening point.

The aforementioned glasses have been fabricated and reported by [41]. The Sellmeier equation and coefficients of

TABLE 2. Sellmeier coefficients of SF57 and LLF1.

Glass	Sellmeier Coefficients	
SF57	P1	1.81651371
	P2	0.428893641
	P3	1.07186278
	Q1	0.0143704198
	Q2	0.0592801172
	Q3	121.419942
LLF1	X1	1.21640125
	X2	0.13366454
	X3	0.883399468
	Y1	0.00857807248
	Y2	0.0420143003
	Y3	107.59306

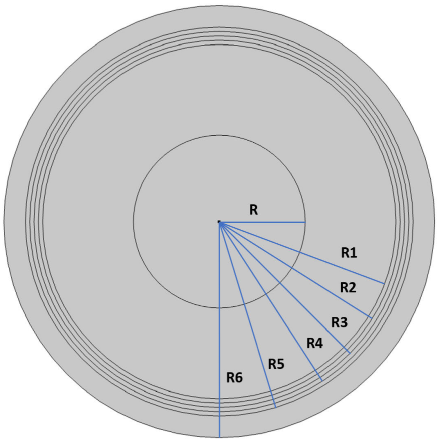

FIGURE 1. Schematic of proposed ring-core Bragg Fiber.

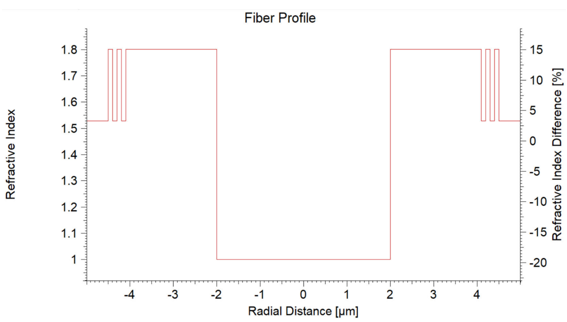

FIGURE 2. Index Profile of proposed ring-core Bragg Fiber.

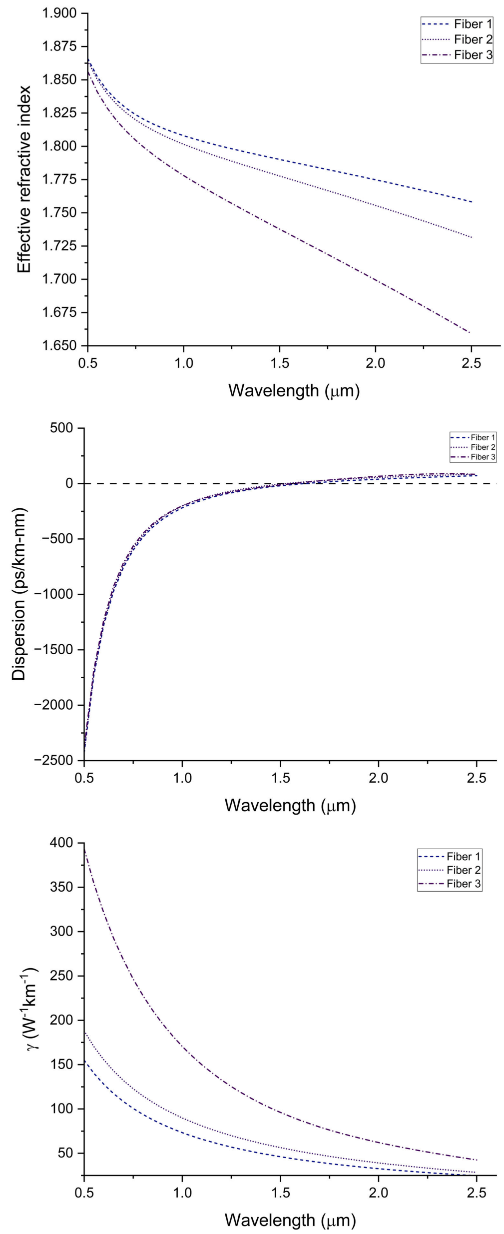

FIGURE 3. (a). Effective refractive index (b). Dispersion profile and (c). Nonlinearity variation of the three fibers.

both the glasses are presented in the following Eq. (1) and Table 2, respectively [40], [42].

$$n^2 - 1 = \sum_{i=1}^{3} \frac{P_i(X_i)\lambda^2}{\lambda^2 - Q_i(Y_i)} \tag{1}$$

A. DESIGN OPTIMIZATION

Three fibers were initially included for optimization to achieve high nonlinearity and for the careful tailoring of dispersion to achieve a ZDW near pump wavelength, as well as to achieve the maximum OAM modes. Further, adding more rings would reduce the leaking of radiation that might happen due to quantum tunneling and only few layers would aid in achieving very low losses and hence we have restricted our discussion to 4 rings in the exterior geometry [43]. Next, the diameter of the central air hole was taken to be the primary parameter which controls the optimization objectives. The three fibers are named Fiber 1, Fiber 2 and Fiber 3 for feasibility, and these names will be further used throughout the manuscript.

The design specifications of the three fibers are presented in Table 3. As shown in the table, the central air hole radius of Fiber 1 to Fiber 3 is increased by 1 μm. This variation assists in achieving an increased nonlinearity due to decrease in effective area and a ZDW tailoring as per need.

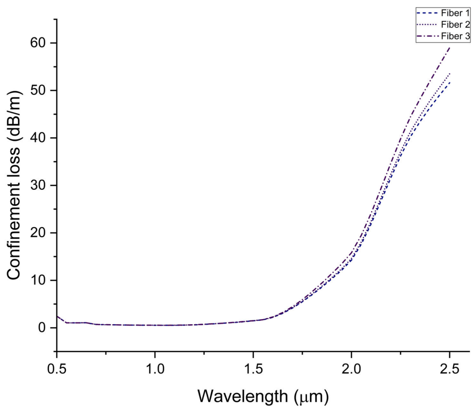

FIGURE 4. Confinement losses for Fibers 1, 2 and 3.

TABLE 3. Geometrical parameters of fibers (All values in μm).

Design parameter	Fiber 1	Fiber 2	Fiber 3
Central Air Hole	1.0	2.0	3.0
R1	4.1	4.1	4.1
R2	4.2	4.2	4.2
R3	4.3	4.3	4.3
R4	4.4	4.4	4.4
R5	4.5	4.5	4.5
R6	5.0	5.0	5.0

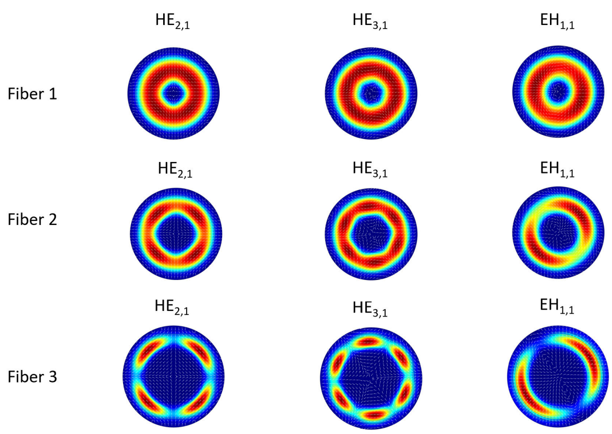

FIGURE 5. $HE_{2,1}$, $HE_{3,1}$ and $EH_{1,1}$ modes in the Fibers 1, 2 and 3.

Dispersion is calculated using the Eq. (2) [44]. Effective area, described in Eq. (3) [21] and nonlinearity have an inverse relationship with each other. Hence, the study of effective area becomes very significant while considering nonlinear applications. The equation supporting this relation is given by Eq. (4) [45], where nonlinear refractive index of the material is denoted by n_2. The n_2 for the proposed SF57 is 4.1×10^{-19} m^2/W [42].

$$D = -\frac{\lambda}{c} \frac{d^2 Re[n_{eff}]}{d\lambda^2} \tag{2}$$

$$A_{eff} = \frac{(\iint |E(x,y)|^2 dxdy)^2}{\iint |E(x,y)|^4 dxdy} \tag{3}$$

$$\gamma = \frac{2\pi n_2}{\lambda A_{eff}} \tag{4}$$

Fig. 3(a) to 3(c) demonstrate the change in effective refractive index (N_{eff}), dispersion (D) and nonlinearity (γ) for the three fibers for the wavelengths from 0.5 μm to 2.5 μm for the $HE_{1,1}$ mode. In the Fig. 3(a), the effective refractive index is decreasing in each of the three fibers for higher wavelengths due to tighter field confinement in the core region with increase in wavelength. The highest index is achieved for Fiber 1 with the lowest central air hole radius, which effectively has the highest core area with the high index material thus increasing the effective refractive index. For Fibers 2 and 3, the central air hole radius increases causing the ring-core to shrink and thus reducing the effective refractive index. Fig. 3(b) shows the dispersion versus wavelength curve for the three fibers. The fiber has been engineered so that a ZDW is achieved for the three fibers at approximately 1.55 μm, which is the wavelength at which OAM mode transmission is tested. In the Fig. 3(c), the change in nonlinearity with the wavelength is demonstrated. The reason for the high nonlinearity for the Fiber 3 is due to the lower effective area as compared to Fibers 1 and 2. The nonlinearity achieved for Fiber 3 at 1.55 μm is 91.51 W^{-1}km^{-1}.

Bulk loss of SF57 is taken to be 1.6 dB/m [28]. Further, the confinement losses in the three fibres are depicted in Fig. 4 for $HE_{1,1}$ mode. For the three fibers, the losses we report are 1.68 dB/m, 1.69 dB/m and 1.72 dB/m at 1.55 μm. The calculations for the confinement losses are performed using the imaginary part of the effective refractive index as shown in Eq. (5) [46].

$$L_C = 8.686 \cdot k_0 \cdot Im(n_{eff}) \tag{5}$$

III. OAM MODES

A few vector modes obtained in the three fibers such as $HE_{2,1}$, $HE_{3,1}$ and $EH_{1,1}$ are plotted in Fig. 5. Further in Fig. 6, the OAM mode generation and transmission has been shown for the modes $HE_{2,1}$, $HE_{4,1}$ and $HE_{2,2}$ in the Fibers 1, 2 and 3 respectively as per Eq. (6) and Eq. (7) at 1.55 μm. Remaining OAM modes are listed in Table 4. The OAM modes are the result of the combination of HE/EH even and odd eigenvectors. The following equations govern the process of OAM mode formation [47], [48].

$$\left\{ \begin{array}{l} OAM^{\pm}_{\pm l,m} = HE^{even}_{l+1,m} \pm jHE^{odd}_{l+1,m} \\ OAM^{\mp}_{\pm l,m} = EH^{even}_{l-1,m} \pm jEH^{odd}_{l-1,m} \end{array} \right\}; \quad (l > 1) \tag{6}$$

$$\left\{ \begin{array}{l} OAM^{\pm}_{\pm 1,m} = HE^{even}_{2,m} \pm jHE^{odd}_{2,m} \\ OAM^{\mp}_{\pm 1,m} = TM_{0,m} \pm jTE_{0,m} \end{array} \right\}; \quad (l = 1) \tag{7}$$

From Fig. 6, for the $HE_{2,1}$ mode in Fiber 1, $OAM^{\pm}_{\pm 1,1}$ is obtained. Similarly, in the Fibers 2 and 3, $OAM^{\pm}_{\pm 3,1}$ and $OAM^{\pm}_{\pm 1,2}$ are obtained for $HE_{4,1}$ and $HE_{2,2}$ modes respectively.

From Table 4, a total of 16 OAM modes, 18 OAM modes and 22 OAM modes are obtained in the Fibers 1, 2 and 3 respectively.

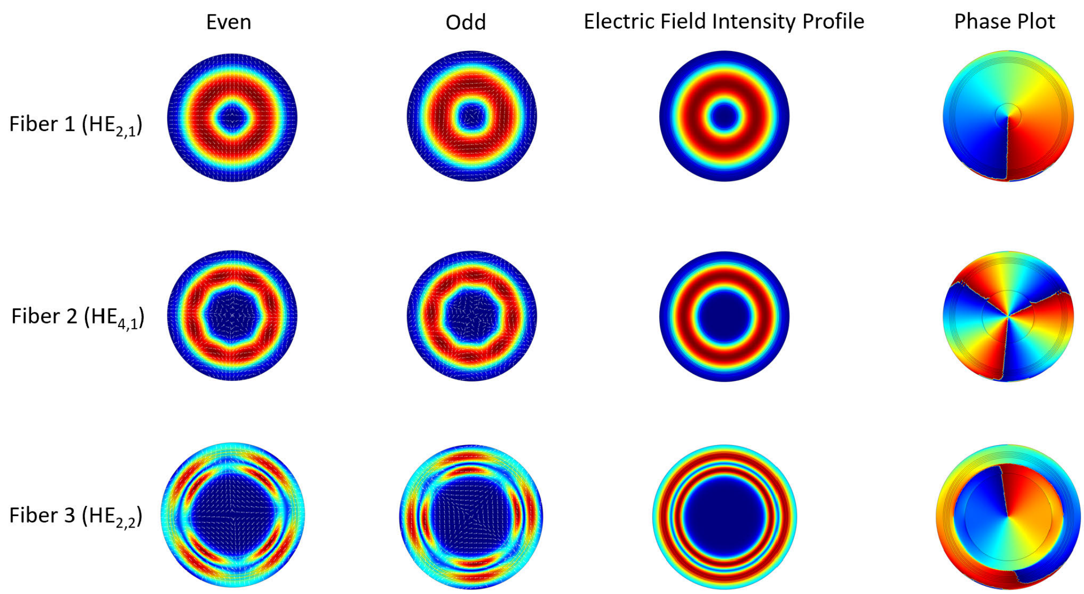

FIGURE 6. OAM mode generation and transmission for $HE_{2,1}$ in Fiber 1, $HE_{4,1}$ in Fiber 2 and $HE_{2,2}$ in Fiber 3.

TABLE 4. OAM modes obtained in Fibers 1, 2 and 3.

Fiber	OAM modes
Fiber 1	$OAM^{\pm}_{\pm1,1}$, $OAM^{\pm}_{\pm1,2}$, $OAM^{\pm}_{\pm2,1}$, $OAM^{\pm}_{\pm2,1}$, $OAM^{\pm}_{\pm3,1}$, $OAM^{\pm}_{\pm3,1}$, $OAM^{\pm}_{\pm4,1}$, $OAM^{\pm}_{\pm4,1}$, $OAM^{\pm}_{\pm5,1}$, $OAM^{\pm}_{\pm5,1}$, $OAM^{\pm}_{\pm6,1}$, $OAM^{\pm}_{\pm6,1}$, $OAM^{\pm}_{\pm7,1}$, $OAM^{\pm}_{\pm7,1}$, $OAM^{\pm}_{\pm8,1}$, $OAM^{\pm}_{\pm8,1}$
Fiber 2	$OAM^{\pm}_{\pm1,1}$, $OAM^{\pm}_{\pm1,2}$, $OAM^{\pm}_{\pm2,1}$, $OAM^{\pm}_{\pm2,1}$, $OAM^{\pm}_{\pm3,1}$, $OAM^{\pm}_{\pm3,1}$, $OAM^{\pm}_{\pm4,1}$, $OAM^{\pm}_{\pm4,1}$, $OAM^{\pm}_{\pm5,1}$, $OAM^{\pm}_{\pm5,1}$, $OAM^{\pm}_{\pm6,1}$, $OAM^{\pm}_{\pm6,1}$, $OAM^{\pm}_{\pm7,1}$, $OAM^{\pm}_{\pm7,1}$, $OAM^{\pm}_{\pm8,1}$, $OAM^{\pm}_{\pm8,1}$, $OAM^{\pm}_{\pm9,1}$, $OAM^{\pm}_{\pm9,1}$
Fiber 3	$OAM^{\pm}_{\pm1,1}$, $OAM^{\pm}_{\pm1,2}$, $OAM^{\pm}_{\pm2,1}$, $OAM^{\pm}_{\pm2,1}$, $OAM^{\pm}_{\pm3,1}$, $OAM^{\pm}_{\pm3,1}$, $OAM^{\pm}_{\pm4,1}$, $OAM^{\pm}_{\pm4,1}$, $OAM^{\pm}_{\pm5,1}$, $OAM^{\pm}_{\pm5,1}$, $OAM^{\pm}_{\pm6,1}$, $OAM^{\pm}_{\pm6,1}$, $OAM^{\pm}_{\pm7,1}$, $OAM^{\pm}_{\pm7,1}$, $OAM^{\pm}_{\pm8,1}$, $OAM^{\pm}_{\pm8,1}$, $OAM^{\pm}_{\pm9,1}$, $OAM^{\pm}_{\pm9,1}$, $OAM^{\pm}_{\pm10,1}$, $OAM^{\pm}_{\pm10,1}$, $OAM^{\pm}_{\pm11,1}$, $OAM^{\pm}_{\pm11,1}$

IV. SUPERCONTINUUM GENERATION

GNLSE is used to mathematically analyze the ultrashort pulse propagation in the aforementioned fibres [36].

The equation is a combination of linear as well as nonlinear components.

$$\frac{\partial A}{\partial z} = \left(\hat{D} + \hat{N}\right) A \tag{8}$$

Here $\hat{D}$ accounts for all of the dispersion terms, and $\hat{N}$ considers the nonlinear propagation effects of the pulse. These terms are further explained as:

$$\hat{D} = -\frac{\alpha}{2} + \left(\sum_{n\geq 2} \frac{i^{n+1}}{n!} \beta_n \frac{\partial^n}{\partial T^n}\right) \tag{9}$$

$$\hat{N} = i\gamma \left(1 + \frac{i}{\omega_0} \frac{\partial}{\partial t}\right) \int_{-\infty}^{\infty} R(T') |A(z, T - T')|^2 dT' \tag{10}$$

From Eq. (9) and (10), α is the fiber loss coefficient, optical field envelope is denoted by $A(z, t)$, z is the distance, time is denoted by T, β_n is the propagation constant's derivative of the n^{th} order and γ is the nonlinear coefficient.

The mathematical way to show the response of nonlinear function $R(t)$ is shown as

$$R(T) = (1 - f_r)\delta(T) + f_r h_r(T) \tag{11}$$

In Eq. (11), $\delta(T)$ and h_r(T) are denoted as instantaneous electronic response and delayed Raman response respectively.

$f_r = 0.1$ for SF57 [49], therefore h_r is shown as:

$$h_r(T) = \frac{\tau_1^2 + \tau_2^2}{\tau_1 \tau_2^2} exp\left(\frac{-t}{\tau_2}\right) sin\left(\frac{t}{\tau_1}\right) \tag{12}$$

For SF57, τ_1 and τ_2 are 5.5 fs and 32.0 fs respectively [50].

GNLSE has been calculated involving the split-step Fourier method [51].

The laser used in the simulation has been modeled after Origami - 15HP laser as a hyperbolic secant pulse at an average power of about 57 mW, and time period, $T_{FWHM} = 200$ fs. Further, 50 MHz is the pulse repetition rate and the fiber length is 20 cm at an operating wavelength of 1.55 μm.

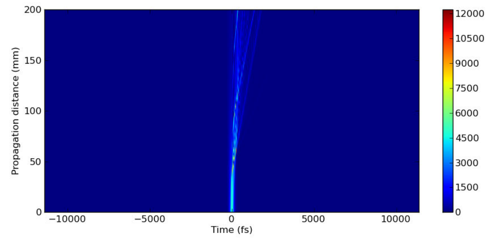

(a)

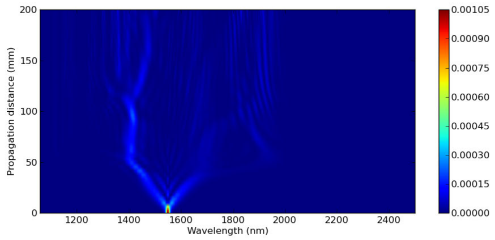

(b)

FIGURE 7. **(a) Temporal and (b) Spatial domain evolution of 5 kW, 200 fs, 1.55 μm pulse in 20 cm RC-BF (Fiber 3).**

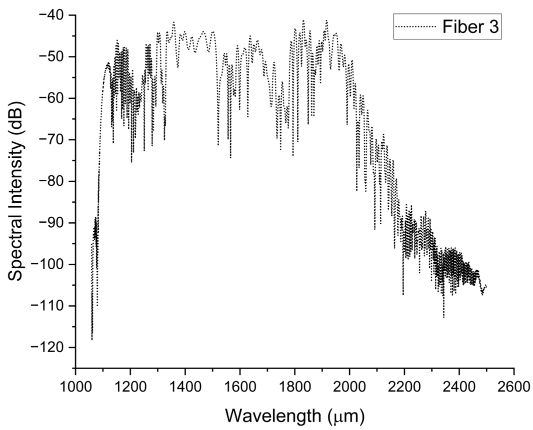

FIGURE 8. **SC spectra at 20 cm fiber length.**

The equation describing the hyperbolic secant function is as follows [41]:

$$A(z=0,t) = \sqrt{P_0} sech\left(\frac{t}{t_0}\right) exp\left(-i\frac{C}{2}\frac{t^2}{t_0^2}\right)$$
$$t_0 = t_{FWHM}/1.7627 \qquad (13)$$

Here the peak power of the pulse is $P_0 = 5$ kW.

Supercontinuum spectrum for Fiber 3 is being shown in Fig. 7 because it has shown to transmit the highest number of OAM modes at 1.55 μm which is also the input pump wavelength. Fig. 7 (a) and 7 (b) demonstrate the evolution of the pulse through Fiber 3 of length 20 cm. High fiber nonlinearity and the position and properties of the input pulse with respect to ZDW significantly affect the SC generation. The pump wavelength is 1.55 μm and is close to ZDW of the fiber. Initially symmetric broadening is observed in the fiber. SPM is responsible for this uniform broadening. At the ZDW, the GVD parameter β_2 almost becomes negligible and hence the effects of third-order dispersion become prominent. Along with third-order dispersion, Raman scattering is also significant in spectral broadening and together they perturb the pulse evolution and initiate the formation of soliton fission [52]. Further the spectrum gets transferred to the anomalous dispersion region and the effects of soliton dynamics are observed here. Higher order dispersion effects are much more significant in PCFs than in conventional fibers and cause the unstable solitons to break and form fundamental solitons. This is termed as soliton decay. The solitons emit nonsolitonic radiation which are shifted towards the blue region of the spectrum to maintain their shape. The wavelength at which the nonsolitonic radiation is emitted relies on how well the phases match. The solitons, however get shifted to the infrared part of spectrum to achieve stability. After this, an interplay of complex processes such as stimulated Raman scattering and dispersion of the fiber cause the spectrum to broaden. These processes are also significant in achieving a flat supercontinuum [53].

The SC spectra of the pulse at 200 mm in Fiber 3 is shown in Fig. 8. The SC obtained spans from 1087 nm to 2024 nm with a flatness of 35 dB.

V. CONCLUSION

This work presents a ring-core Bragg Fiber designed with a combination of Schott flint glasses, SF57 and LLF1. Moreover, the fabrication of the Bragg fiber is also simple. After careful optimization, the fiber is capable of supporting 22 OAM modes propagating at 1.55 μm and producing a very flat supercontinuum spectra of 35 dB from 1087 - 2024 nm by launching a chirp-free hyperbolic secant pulse of having a pulse width of 200 fs with a maximum power of 5 kW. The SC spectra extends in the mentioned wavelength range with a flat spectrum. Due to the higher nonlinear refractive index of the glasses used in the design, it is more suitable for nonlinear applications in comparison to silica and offers low loss in comparison to chalcogenide, tellurite, and other infrared glasses. This makes them suitable for both applications mentioned in the paper. Furthermore, soft glass fibers are also easier to fabricate when compared to chalcogenide, tellurite, and other infrared glasses due to high glass transition temperature, low thermal expansion coefficient, and high thermal conductivity.

REFERENCES

[1] Y. Ren, L. Li, Z. Wang, S. M. Kamali, E. Arbabi, A. Arbabi, Z. Zhao, G. Xie, Y. Cao, N. Ahmed, Y. Yan, C. Liu, A. J. Willner, S. Ashrafi, M. Tur, A. Faraon, and A. E. Willner, "Orbital angular momentum-based space division multiplexing for high-capacity underwater optical communications," *Sci. Rep.*, vol. 6, no. 1, pp. 1–10, Sep. 2016.

[2] Y. Wang, Y. Lu, C. Bao, W. Geng, Y. Fang, B. Mao, Z. Wang, Y. Liu, H. Huang, Y. Ren, Z. Pan, and Y. Yue, "Hollow ring-core photonic crystal fiber with > 500 OAM modes over 360-nm communications bandwidth," *IEEE Access*, vol. 9, pp. 66999–67005, 2021.

[3] F. A. Al-Zahrani and M. A. Kabir, "Ring-core photonic crystal fiber of terahertz orbital angular momentum modes with excellence guiding properties in optical fiber communication," *Photonics*, vol. 8, no. 4, p. 122, 2021.

[4] J. Wang, J.-Y. Yang, I. M. Fazal, N. Ahmed, Y. Yan, H. Huang, Y. Ren, Y. Yue, S. Dolinar, M. Tur, and A. E. Willner, "Terabit free-space data transmission employing orbital angular momentum multiplexing," *Nature Photon.*, vol. 6, no. 7, pp. 488–496, Jul. 2012.

[5] L. Yan, P. Kristensen, and S. Ramachandran, "Vortex fibers for STED microscopy," *APL Photon.*, vol. 4, no. 2, Feb. 2019, Art. no. 022903.

[6] D. Bacco, D. Cozzolino, B. Da Lio, Y. Ding, K. Rottwitt, and L. K. Oxenløwe, "Quantum communication with orbital angular momentum," in *Proc. 22nd Int. Conf. Transparent Opt. Netw. (ICTON)*, Jul. 2020, pp. 1–4.

[7] M. Krenn, M. Malik, M. Erhard, and A. Zeilinger, "Orbital angular momentum of photons and the entanglement of Laguerre–Gaussian modes," *Phil. Trans. Roy. Soc. A, Math., Phys. Eng. Sci.*, vol. 375, no. 2087, 2017, Art. no. 20150442.

[8] V. Bobkova, J. Stegemann, R. Droop, E. Otte, and C. Denz, "Optical grinder: Sorting of trapped particles by orbital angular momentum," *Opt. Exp.*, vol. 29, no. 9, pp. 12967–12975, Apr. 2021.

[9] D. Cojoc, V. Garbin, E. Ferrari, L. Businaro, F. Romanato, and E. D. Fabrizio, "Laser trapping and micro-manipulation using optical vortices," *Microelectronic Eng.*, vols. 78–79, pp. 125–131, Mar. 2005.

[10] F. Pang, H. Zheng, H. Liu, J. Yang, N. Chen, Y. Shang, S. Ramachandran, and T. Wang, "The orbital angular momentum fiber modes for magnetic field sensing," *IEEE Photon. Technol. Lett.*, vol. 31, no. 11, pp. 893–896, Jun. 1, 2019.

[11] A. Dubietis, A. Couairon, and G. Genty, "Supercontinuum generation: Introduction," *JOSA B*, vol. 36, no. 2, pp. SG1–SG3, 2019.

[12] J. M. Dudley, G. Genty, and S. Coen, "Supercontinuum generation in photonic crystal fiber," *Rev. Modern Phys.*, vol. 78, p. 1135, Oct. 2006.

[13] X. Wang, T. Hamanaka, N. Wada, and K.-I. Kitayama, "Dispersion-flattened-fiber based optical thresholder for multiple-access-interference suppression in OCDMA system," *Opt. Exp.*, vol. 13, no. 14, pp. 5499–5505, 2005.

[14] G. Humbert, W. Wadsworth, S. Leon-Saval, J. Knight, T. Birks, P. S. J. Russell, M. Lederer, D. Kopf, K. Wiesauer, E. Breuer, and D. Stifter, "Supercontinuum generation system for optical coherence tomography based on tapered photonic crystal fibre," *Opt. Exp.*, vol. 14, no. 4, pp. 1596–1603, 2006.

[15] A. Ghanbari, A. Kashaninia, A. Sadr, and H. Saghaei, "Supercontinuum generation for optical coherence tomography using magnesium fluoride photonic crystal fiber," *Optik*, vol. 140, pp. 545–554, Jul. 2017.

[16] S. Sato, Y. Kozawa, and T. Nakamura, "Generation of white-light supercontinuum with axially symmetric polarization," in *High Intensity Lasers and High Field Phenomena*. Washington, DC, USA: Optica Publishing Group, 2011.

[17] C. F. Kaminski, J. Hult, and T. Laurila, "Supercontinuum radiation for optical sensing," in *Proc. Conf. Lasers Electro-Optics*. Washington, DC, USA: Optical Society of America, 2010, pp. 1–2.

[18] A. Apolonski, B. Povazay, A. Unterhuber, W. Drexler, W. J. Wadsworth, J. C. Knight, and P. S. J. Russell, "Spectral shaping of supercontinuum in a cobweb photonic-crystal fiber with sub-20-fs pulses," *JOSA B*, vol. 19, no. 9, pp. 2165–2170, 2002.

[19] M. Tiwari and V. Janyani, "Two-octave spanning supercontinuum in a soft glass photonic crystal fiber suitable for 1.55 μm pumping," *J. Lightw. Technol.*, vol. 29, no. 23, pp. 3560–3565, Oct. 10, 2011.

[20] H. Li, G. Ren, Y. Lian, B. Zhu, M. Tang, Y. Zhao, and S. Jian, "Broadband orbital angular momentum transmission using a hollow-core photonic bandgap fiber," *Opt. Lett.*, vol. 41, no. 15, pp. 3591–3594, 2016.

[21] W. Tian, H. Zhang, X. Zhang, L. Xi, W. Zhang, and X. Tang, "A circular photonic crystal fiber supporting 26 OAM modes," *Opt. Fiber Technol.*, vol. 30, pp. 184–189, Jul. 2016.

[22] D. Vigneswaran, M. S. M. Rajan, B. Biswas, A. Grover, K. Ahmed, and B. K. Paul, "Numerical investigation of spiral photonic crystal fiber (S-PCF) with supporting high order OAM modes propagation for space division multiplexing applications," *Opt. Quantum Electron.*, vol. 53, no. 2, pp. 1–11, Feb. 2021.

[23] N. A. Mortensen, "Effective area of photonic crystal fibers," *Opt. Exp.*, vol. 10, no. 7, pp. 341–348, 2002.

[24] V. R. K. Kumar, A. George, J. Knight, and P. S. J. Russell, "Tellurite photonic crystal fiber," *Opt. Exp.*, vol. 11, no. 20, pp. 2641–2645, 2003.

[25] E. F. Chillcce, C. M. B. Cordeiro, L. C. Barbosa, and C. H. B. Cruz, "Tellurite photonic crystal fiber made by a stack-and-draw technique," *J. Non-Crystalline Solids*, vol. 352, nos. 32–35, pp. 3423–3428, Sep. 2006.

[26] M. R. Karim, H. Ahmad, and B. M. A. Rahman, "All-normal dispersion chalcogenide PCF for ultraflat mid-infrared supercontinuum generation," *IEEE Photon. Technol. Lett.*, vol. 29, no. 21, pp. 1792–1795, Nov. 1, 2017.

[27] A. B. Khalifa, A. B. Salem, and R. Cherif, "Multimode supercontinuum generation in As_2S_3 chalcogenide photonic crystal fiber," in *Frontiers in Optics*. Washington, DC, USA: Optica Publishing Group, 2018, Paper JTu2A-18.

[28] P. Petropoulos, H. Ebendorff-Heidepriem, V. Finazzi, R. Moore, K. Frampton, D. Richardson, and T. Monro, "Highly nonlinear and anomalously dispersive lead silicate glass holey fibers," *Opt. Exp.*, vol. 11, no. 26, pp. 3568–3573, 2003.

[29] G. Sobon, M. Klimczak, J. Sotor, K. Krzempek, D. Pysz, R. Stepien, T. Martynkien, K. M. Abramski, and R. Buczynski, "Infrared supercontinuum generation in soft-glass photonic crystal fibers pumped at 1560 nm," *Opt. Mater. Exp.*, vol. 4, no. 1, pp. 7–15, 2014.

[30] F. Belli, A. Abdolvand, W. Chang, J. C. Travers, and P. S. J. Russell, "Vacuum-ultraviolet to infrared supercontinuum in hydrogen-filled photonic crystal fiber," *Optica*, vol. 2, no. 4, pp. 292–300, 2015.

[31] C. L. Huang, M. S. Liao, W. J. Bi, X. Li, L. L. Hu, L. Zhang, L. F. Wang, G. S. Qin, T. F. Xue, D. P. Chen, and W. Q. Gao, "Ultraflat, broadband, and highly coherent supercontinuum generation in all-solid microstructured optical fibers with all-normal dispersion," *Photon. Res.*, vol. 6, no. 6, pp. 601–608, Jun. 2018.

[32] J. Y. Y. Leong, P. Petropoulos, J. H. V. Price, H. Ebendorff-Heidepriem, S. Asimakis, R. C. Moore, K. E. Frampton, V. Finazzi, X. Feng, T. M. Monro, and D. J. Richardson, "High-nonlinearity dispersion-shifted lead-silicate holey fibers for efficient 1-μm pumped supercontinuum generation," *J. Lightw. Technol.*, vol. 24, no. 1, pp. 183–190, Jan. 1, 2006.

[33] A. Agrawal, N. Kejalakshmy, B. M. A. Rahman, and K. T. V. Grattan, "Soft glass equiangular spiral photonic crystal fiber for supercontinuum generation," *IEEE Photon. Technol. Lett.*, vol. 21, no. 22, pp. 1722–1724, Nov. 2009.

[34] G. Vienne, Y. Xu, C. Jakobsen, H.-J. Deyerl, J. B. Jensen, T. Sørensen, T. P. Hansen, Y. Huang, M. Terrel, R. K. Lee, and N. A. Mortensen, "Ultra-large bandwidth hollow-core guiding in all-silica Bragg fibers with nano-supports," *Opt. Exp.*, vol. 12, no. 15, pp. 3500–3508, 2004.

[35] A. Nandam and W. Shin, "Spiral photonic crystal fiber structure for supporting orbital angular momentum modes," *Optik*, vol. 169, pp. 361–367, Sep. 2018.

[36] Y. Wang, Y. Fang, W. Geng, J. Jiang, Z. Wang, H. Zhang, C. Bao, H. Huang, Y. Ren, Z. Pan, and Y. Yue, "Beyond two-octave coherent OAM supercontinuum generation in air-core As_2S_3 ring fiber," *IEEE Access*, vol. 8, pp. 96543–96549, 2020.

[37] X. Bai, H. Chen, Y. Zhuang, and H. Cao, "A new type Bragg fiber for supporting 50 orbital angular momentum modes," *Optik*, vol. 219, Oct. 2020, Art. no. 165153.

[38] J. Zheng, W. Lei, Y. Qin, H. Zou, K. Yu, and W. Wei, "Highly nonlinear dispersion-flattened high-index-core Bragg fibres for supercontinuum generation," *J. Modern Opt.*, vol. 66, no. 20, pp. 2008–2014, Nov. 2019.

[39] G. Tao, H. Ebendorff-Heidepriem, A. M. Stolyarov, S. Danto, J. V. Badding, Y. Fink, J. Ballato, and A. F. Abouraddy, "Infrared fibers," *Adv. Opt. Photon.*, vol. 7, pp. 379–458, Apr. 2015.

[40] Schott. (2022). *Schott Glass Datasheets on Interactive Abbe Diagram*. [Online]. Available: https://www.schott.com/en-in/interactive-abbe-diagram

[41] X. Feng, G. M. Ponzo, F. Poletti, A. Camerlingo, F. Parmigiani, M. N. Petrovich, P. Petropoulos, N. M. White, W. H. Loh, and D. J. Richardson, "A single-mode, high index-contrast, lead silicate glass fibre with high nonlinearity, broadband near-zero dispersion at telecommunication wavelengths," in *Proc. 36th Eur. Conf. Exhib. Opt. Commun.*, Sep. 2010, pp. 1–3.

[42] X.-P. Zhu, S.-G. Li, Y. Du, Y. Han, W.-Q. Zhang, Y.-L. Ruan, H. Ebendorff-Heidepriem, S. Afshar, and T. M. Monro, "High stability supercontinuum generation in lead silicate SF57 photonic crystal fibers," *Chin. Phys. B*, vol. 22, no. 1, Jan. 2013, Art. no. 014215.

[43] S. G. Johnson, M. Ibanescu, M. Skorobogatiy, O. Weisberg, T. D. Engeness, M. Soljačić, S. A. Jacobs, J. Joannopoulos, and Y. Fink, "Low-loss asymptotically single-mode propagation in large-core omniguide fibers," *Opt. Exp.*, vol. 9, no. 13, pp. 748–779, Dec. 2001.
[44] Z. Geng, N. Wang, K. Li, H. Kang, X. Xu, X. Liu, W. Wang, and H. Jia, "A photonic crystal fiber with large effective refractive index separation and low dispersion," *PLoS ONE*, vol. 15, no. 5, May 2020, Art. no. e0232982.
[45] W. Wang, C. Sun, N. Wang, and H. Jia, "A design of nested photonic crystal fiber with low nonlinear and flat dispersion supporting 30+50 OAM modes," *Opt. Commun.*, vol. 471, Sep. 2020, Art. no. 125823.
[46] I. Amiri, P. Yupapin, and A. N. Z. Rashed, "Mathematical model analysis of dispersion and loss in photonic crystal fibers," *J. Opt. Commun.*, vol. 44, no. 1, pp. 139–144, Jan. 2023.
[47] F. A. Al-Zahrani and M. Mehedi Hassan, "Enhancement of OAM and LP modes based on double guided ring fiber for high capacity optical communication," *Alexandria Eng. J.*, vol. 60, no. 6, pp. 5065–5076, Dec. 2021.
[48] Y. Yu, Y. Lian, Q. Hu, L. Xie, J. Ding, Y. Wang, and Z. Lu, "Design of PCF supporting 86 OAM modes with high mode quality and low nonlinear coefficient," *Photonics*, vol. 9, no. 4, p. 266, Apr. 2022.
[49] X. Zhang, "Study of supercontinuum and high repetition rate short pulse generation," Ph.D. dissertations, Univ. Connecticut, Connecticut, 2018.
[50] X. Zhang, H. Hu, W. Li, and N. K. Dutta, "Supercontinuum generation in dispersion-varying microstructured optical fibers," in *Proc. SPIE*, vol. 9834, 2016, pp. 78–84.
[51] M. Kiroriwal and P. Singal, "Numerical analysis on the supercontinuum generation through $Al_{0.24}Ga_{0.76}As$ based photonic crystal fiber," *Sādhanā*, vol. 46, no. 3, pp. 1–8, Sep. 2021.
[52] S. Zhang, X. Yang, F. Lu, Y. Gong, and X. Meng, "Supercontinuum generation in photonic crystal fibers with a normal dispersion pump pulse near the zero-dispersion wavelength," *Opt. Eng.*, vol. 47, no. 7, Jul. 2008, Art. no. 075005.
[53] F. Poli, A. Cucinotta, and S. Selleri, *Photonic Crystal Fibers: Properties and Applications*, vol. 102. Dordrecht, The Netherlands: Springer, 2007.

AMOGH A. DYAVANGOUDAR is currently pursuing the bachelor's degree in electronics and communication engineering with Manipal University Jaipur. He is also involved in the designing and modeling of photonic crystal fibers for orbital angular momentum mode propagation and super continuum generation. He has presented his work in several international conferences.

MAYUR KUMAR CHHIPA is currently working on 2-D photonic crystal-based passive devices, photonic band gap structures, photonic crystal micro/nano ring resonator structures, devices for CWDM/DWDM applications and optical communication networking systems, and PIC. He has also designed some structures based on optical switch, optical sensors, and optical logic gates.

ANKUR SAHARIA (Member, IEEE) received the M.Tech. and Ph.D. degrees in ECE and in integrated optics from MNIT Jaipur. He is currently an Assistant Professor with the Department of ECE, Manipal University Jaipur. He has more than eight years of professional experience in various colleges and universities of repute. He has published numerous research papers in reputed journals and conferences, and many book chapters. He has guided many projects during his teaching tenure as a faculty member. He has received travel grant to attend FIO-LS 2019. He is a reviewer for many reputed journals and conference due to his contribution to research. He has received many awards and recognition for his research work recently at the university level. He is a Senior Member of Optica and a member of SPIE, India. His current research interests include micro/nanostructure, photonic devices, SPR sensors, photonic ICs, nonlinear optics, and photonic crystal fibers.

YASEERA ISMAIL received the Master of Science degree (cum laude) in physics from the Council for Scientific and Industrial Research (CSIR), Pretoria, South Africa, in 2011, and the Ph.D. degree from the Quantum Research Group, University of KwaZulu-Natal, in 2015. She is currently a Postdoctoral Researcher with the University of KwaZulu-Natal. Her current research interests include quantum optics in particular focusing on quantum communication and the development of the quantum enabled technologies. She is also working in the experimental development of South Africa's first cold atoms system. She has been involved in several outreach programs which includes the Public Understanding of Laser Science and Engineering (PULSE) Outreach Program, from 2009 to 2010. She has been judging the Eskom Expo for Young Scientist and Engineers, since 2012. She was invited to represent South Africa at the UNESCO International Year of Light Opening Ceremony, in 2015, and have contributed to the Bright Futures Optics and Photonics news for careers in optics. She is also a member of the Optica Early Career Program and awarded a TechWomen Emerging Leader, in 2016.

FRANCESCO PETRUCCIONE received the degree in physics from the University of Freiburg im Breisgau, the Ph.D. degree, in 1988, and the Habilitation (Dr. rer. nat. habil.) degree, in 1994. In 2004, he was appointed as a Professor in theoretical physics with the University of KwaZulu-Natal (UKZN), Durban, South Africa. In 2007, he was granted the South African Research Chair for Quantum Information Processing and Communication. He has been the Pro-Vice-Chancellor of Big Data and Informatics with UKZN. Currently, he is the Interim Director of the National Institute for Theoretical and Computational Sciences. Since May 2022, he has been a Professor in quantum computing with Stellenbosch University and a Fractional Professor with UKZN. He is an elected member of the Academy of Sciences of South Africa, a fellow of the Royal Society of South Africa, the African Academy of Sciences, and the University of KwaZulu-Natal. He has published more than 250 articles in refereed scientific journals. He is the coauthor of a monograph on *The Theory of Open Quantum Systems* (more than 10000 citations according to Google Scholar), that was published, in 2002, reprinted as paperback, in 2007, and translated in Russian. In 2018, he published a monograph (with Maria Schuld) on *Supervised Learning with Quantum Computers* that was already translated into Japanese. He was published *Machine Learning with Quantum Computers* (Second Extended Edition, 2021). He is an editor of several proceedings volumes and special editions of scientific journals. He is a member of the editorial board of the journals, such as *Open Systems and Information Dynamics*, *Scientific Reports*, and *Quantum Machine Intelligence*.

ANTON V. BOURDINE received the Ph.D. degree from the Povolzhskiy State University of Telecommunications and Informatics (PSUTI), Samara, Russia, in November 2002, and the Doctor of Technical Sciences degree from Ufa State Aviation University (USATU), Ufa, Russia, in December 2013. He embarked upon the career in fiber optics and in telecommunications from LLC Research and Development Company ''CAM,'' Samara, Russia, in 1996, when he was involved as a technician and an engineer in design, installation, mounting, testing, and maintenance both of aerial and underground fiber optic links of WANs, MANs, and LANs for various Russian telecommunication and oil/gas/railway branch companies. In 2003, he became the Head of the Department of Perspective Technologies, ''CAM,'' where he worked until June 2015. He is currently a Professor with the Department of Communication Lines, PSUTI. In 2020, he relocated to Saint-Petersburg and started spin-off of his scientific activity in JSC ''Scientific Production Association State Optical Institute named after Vavilov S. I.'' His research interests include the development of fast and simple methods for the design of novel few-mode optical fibers (FMFs) for long haul links of extra high bit rate new generation networks, design, and fabrication FMFs with extremely enlarged core diameter for short range laser-based data transmission, the research of few-mode effects in sensor applications, including design and fabrication complicated few-mode silica twisted silica microstructured optical fibers with GeO2 multi-cores. He is a fellow of OSA and SPIE, a Senior Member of OSA, and a Regular Member of SPIE. He is a Scientific Advisor of PSUTI SPIE Student Chapter, in 2015.

OLEG G. MOROZOV (Senior Member, IEEE) was born in Kazan Tatarstan, Russia, in October 1960. He received the Ph.D. degree in technics from the Tupolev Aviation Institute, Kazan, in 1987, and the Doctor of Technology degree from Kazan National Research Technical University, Kazan, in 2004. He leads research in microwave photonics, fiber optics sensors, and its interrogation, as a radio engineer and a researcher. He became an Engineer in radiotechnics with the Aviation Institute, in 1983. He was the Head of the Quantum Electronics and Laser Technology Research and Development Laboratory, from 1989 to 1993, and the Head of the TV and Multimedia System Department, from 2005 to 2014. Currently, he is the Head of the Radiophotonics and Microwave Technology Department and the Research and Development Institute of Applied Electrodynamics, Photonics and Live Systems.

VLADIMIR V. DEMIDOV has worked on optical fibers, optical fiber fabrication, silicon compounds, gadolinium compounds, holey fibers, microoptics, nanofabrication, nanoparticles, neodymium, optical design techniques, optical vortices, phosphors, photoluminescence, chirality, crystal morphology, fiber optic sensors, integrated optics, light reflection, light transmission, luminescence, numerical analysis, optical fabrication, optical fiber cladding, and optical fiber losses.

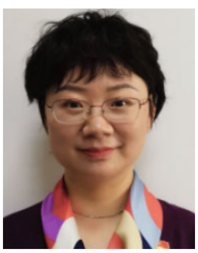

JUAN YIN was born in December 1982. She received the Ph.D. degree, in 2011. She is currently a Professor in experimental physics with USTC. She is also the chief designer of the payload on Micius quantum science satellite. She has been engaged in the experimental study of long-distance entanglement-based quantum physics for a long time. She has published 42 articles in international journals, including five articles in *Nature*, two articles in *Science*, two articles in *Nature Photonics*, one article each in *Nature Physics* and *PNAS*, and nine articles in *Physical Review Letters*. Her publications have been cited more than 2680 times (ISI Web of Science). To further show the impact of her major achievements, her work has been selected for twice annual highlights by Nature as ''Features of the Year 2012,'' ''2017 in news: The science events that shaped the year,'' and three times ''The Top Ten Annual Scientific and Technological Progresses in China'' by the academicians of the Chinese Academy of Science and the Chinese Academy of Engineering. She has won many honors, such as Shanghai Rising-Star of Science and Technology, Anhui Science Foundation for Distinguished Young Scholars, Shanghai Women's Innovation Award, ''2018 Young Faculty Career Award'' of USTC Alumni Foundation, ''Newcomb Cleveland Award'' of AAAS, Outstanding Scientific and Technological Achievement Award (Collective) of CAS, and National ''March 8th Red Flag Bearer.''

GHANSHYAM SINGH (Senior Member, IEEE) received the B.Tech. degree from NIT Silchar, India, and the M.Tech. and Ph.D. degrees in electronics and communication engineering from MNIT Jaipur, India. Currently, he is a Full Professor with the Department of ECE, MNIT Jaipur. He was a Visiting Research Scholar/Professor with Heriot-Watt University Edinburgh, U.K., University of Eastern Finland, Joensuu, and Keio University, Japan. He has published over 150 research articles in peer reviewed journals/conference proceedings. He is a Senior Member of SPIE and OSA and a fellow of OSI and IETE. He was a recipient of the 2017 IEEE Distinguished Lecturer Award of the Photonics Society. He is the Chair (Elect) for OSA TG on Optics in Digital Systems and a member for SPIE Fellowship Committee. He is also serving as the Secretary for IEEE Photonics Society Rajasthan Chapter (PHO36), the Faculty Advisor to OSA, and the IEEE Sensor Council Student Chapters of MNIT Jaipur. In the past, he has joint research collaborations with the researchers from Keio University, Japan, University of Vienna, Austria, LNPU, Ukraine, and Cairo University, Egypt. He is also collaborating on a multi- institutional research project with researchers from the University of KwaZulu-Natal, South Africa, PSUTI Samara, Russia, and University of Science and Technology of China, Shanghai, China, for a BRICS STI Framework Program (2020–2023). His current research interests include micro and nano-structured photonic devices for integrated photonics, and signal processing in optical circuits.

MANISH TIWARI received the Ph.D. degree in ECE and in photonics from MNIT Jaipur. He is currently a Professor and the Head of the Department of ECE, Manipal University Jaipur. He has more than 20 years of professional experience in various colleges and universities of repute. He has published more than 100 research papers in reputed journals and conferences, and eight book chapters. He has also authored and edited more than half a dozen of books. He has also supervised more than 29 projects sponsored by DST Rajasthan. He has been a technical program committee member of many IEEE conferences and a reviewer of IEEE/Elsevier/OSA/Springer/T&F journals. He is on the panel of Traveling Lecturer Program of reputed societies, such as SPIE (USA) and Optica (USA) under which he has delivered invited talks with Tsinghua University, Beijing, ITS, Indonesia, University of KwaZulu-Natal, Durban, South Africa on photonics technologies and career development. His current research interests include micro/nano-structure photonic devices, photonic ICs, fiber optics, numerical modeling, nonlinear optics, and photonic crystal fibers.